J|A|C|S
ARTICLES
Published on Web 02/17/2004

BPA-PC on a Ni(111) Surface: The Interplay between Adsorption Energy and Conformational Entropy for Different Chain-End Modifications

Luigi Delle Site,* Salvador Leon, and Kurt Kremer

Contribution from the Max-Planck-Institute for Polymer Research, Ackermannweg 10, D 55021 Mainz, Germany

Received September 26, 2003; E-mail: dellsite@mpip-mainz.mpg.de

Abstract: We extend a previous dual scale modeling approach for the behavior of polymers near a metal surface to a variety of end groups. Our approach combines a coarse-grained polymer model with ab initio DFT calculations. Such a procedure was applied to a melt of phenolic-like terminated Bisphenol A-polycarbonate (BPA-PC) interacting with a (111) nickel surface (Delle Site, L.; Abrams, C. F.; Alavi, A.; Kremer, K. *Phys. Rev. Lett.* **2002**, *89*, 156103. Abrams, C. F.; Delle Site, L.; Kremer, K. *Phys. Rev. E* **2003**, *67*, 021807). This work extends this study to different chain-end modifications of BPA-PC, *p*-*tert*-butylphenolic, *p*-tetramethylpropylphenolic, and *p*-cumylphenolic. We show how the interplay between adsorption energies and conformational entropy selects different morphologies for the various melts at the interface. Implications of these results for realistic technical materials are finally discussed.

I. Introduction

Surface and interface properties of polymer melts are crucial parameters in many applications of macromolecular materials. The final products in many cases include interfaces of different materials, and the problem of adhesion is often central for the applicability of a given class of systems. Also, before the final product is obtained, in many cases polymers are die cast. For this process, including the final separation of the die cast and the polymer material, the specific interaction of chains with the surfaces can be equally important for the final product as the intrinsic product properties themselves. These problems make a detailed knowledge of specific polymer surface interactions combined with more general statistical mechanical information on the conformations near surfaces highly desirable.

The properties of bulk polymers have been studied experimentally as well as with simulations on different levels of detail throughout past years.[1−5] Besides simulation studies of idealized lattice or continuum bead spring models,[4] a number of studies employing atomistic simulations have been performed.[5] For the latter, only very short times can be reached throughout the simulation, and equilibration is a central challenge. For specific systems, the approaches of Theodorou and co-workers, where chains are broken and reconnected, work quite successfully.[6] For coarse-grained models, a modified approach was recently put forward by Everaers et al.[7] A more global ansatz combines the two levels of description and generates first equilibrated coarse-grained conformations and then reintroduces chemical details.[8,9] There are a number of papers which describe the different ways in which molecular coarse-graining was employed over past years.[10−14] Coarse-graining aims to guarantee that the chain conformations in a simulation sample represent true equilibrium conformations of the specific polymer desired. The global conformational relaxation takes (many) orders of magnitude more in time than any local move. A central feature of coarse-graining is that the models retain only as much unique and relevant information as needed about the specific polymer(s) under investigation, using significantly fewer degrees of freedom (i.e., particles) than is required for full atomistic detail. This also means that the characteristic time step in a simulation increases significantly. Depending on the problem studied, the level of detail can vary widely. Once an equilibrated sample at the coarse-grained level is generated using an appropriate

(1) Delle Site, L.; Abrams, C. F.; Alavi, A.; Kremer, K. *Phys. Rev. Lett.* **2002**, *89*, 156103.
(2) Abrams, C. F.; Delle Site, L.; Kremer, K. *Phys. Rev. E* **2003**, *67*, 021807.
(3) Kremer, K. In *Monte Carlo and Molecular Dynamics of Condensed Matter Systems*; Binder, K., Ciccotti, G., Eds.; Italian Physical Society: Bologna, 1996.
(4) Binder, K. *Monte Carlo and Molecular Dynamics Simulation in Polymer Science*; Oxford University Press: New York, 1995.
(5) Suter, U. W., Monnerie, L., Eds. *Advances in Polymer Science*; Springer-Verlag: New York, 1994; Vol. 116.
(6) Karayiannis, N. C.; Mavrantzas, V. G.; Theodorou, D. N. *Phys. Rev. Lett.* **2002**, *88*, 105503.
(7) Auhl, R.; Everaers, R.; Grest, G. S.; Kremer, K.; Plimpton, S. J. *J. Chem. Phys.* **2003**, *119*, 12718.
(8) Tschöp, W.; Kremer, K.; Batoulis, J.; Bürger, T.; Hahn, O. *Acta Polym.* **1998**, *49*, 61.
(9) Tschöp, W.; Kremer, K.; Hahn, O.; Batoulis, J.; Bürger, T. *Acta Polym.* **1998**, *49*, 75.
(10) Abrams, C. F.; Delle Site, L.; Kremer, K. Multiscale Computer Simulations for Polymeric Materials in Bulk and near Surfaces in Bridging time scales: Molecular Simulations for the next decade. In *Lecture Notes in Physics*; Nielaba, P., Mareschal, M., Ciccotti, G., Eds.; Springer-Verlag: New York, 2002; Vol. 605, p 143 ff.
(11) Baschnagel, J.; Binder, K.; Doruker, P.; Gusev, A.; Hahn, O.; Kremer, K.; Mattice, W. L.; Müller-Plathe, F.; Murat, M.; Paul, W.; Santos, S.; Suter, U. W.; Tries, V. *Adv. Polym. Sci.* **2000**, *152*, 41.
(12) Paul, W.; Binder, K.; Kremer, K. *Macromolecules* **1991**, *24*, 6332.
(13) Kremer, K.; Müller-Plathe, F. *MRS Bull.* **2001**, *26*, 205.
(14) Müller-Plathe, F. *ChemPhysChem.* **2002**, *3*, 754.

10.1021/ja0387406 CCC: $27.50

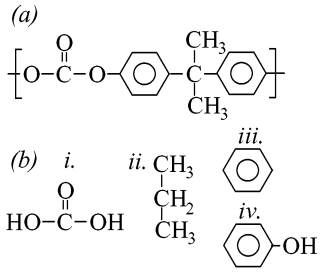

Figure 1. (a) Chemical repeat unit of BPA-PC. (b) Analogous submolecules used in the ab initio study. (i) Carbonic acid analogous of the carbonate group, (ii) propane analogous of the isopropylidene, and (iii) benzene or (iv) phenol analogous of the phenylene.

simulation technique, atomic details can be reintroduced to study atomic-scale properties and processes on, then, appropriately short length and time scales.[9]

For polymer melts next to a surface, the situation is somewhat different. If one is only concerned with generic aspects, the use of the advanced self-consistent field approaches (SCF)[15,16] is sufficient. These calculations have been compared in detail to Monte Carlo as well as molecular dynamics (MD) simulations of idealized models, and the agreement is excellent. Such an approach, however, only can deal with rather global aspects. Differences in the local packing near a surface, which can be huge for different models,[17,18] are beyond the limits of the SCF treatment. The situation becomes more complex if specific interactions with the surface may manipulate conformations close to the surface. There the interplay of chemical structure, local interactions, and global conformations and packing governs the properties. This requires a solid knowledge of each aspect as well as the tools to combine them. In such a context, our focus in recent years has been developing a method for coarse-graining melts of bisphenol-A-polycarbonate (BPA-PC)[8,9,19,20] (Figure 1) as a test case. BPA-PC is the by far most utilized and intensively studied variety of polycarbonate, because of its many valuable material properties, such as high impact strength, ductility, glass transition, and melting temperatures.[21] For example, interesting questions regarding the high ductility of glassy BPA-PC have inspired many experimental,[22−27] simulation,[28−32] and combined experimental/simulation[33,34] studies.

In the present work, we are particularly interested in understanding the (adhesion) behavior of BPA-PC liquids

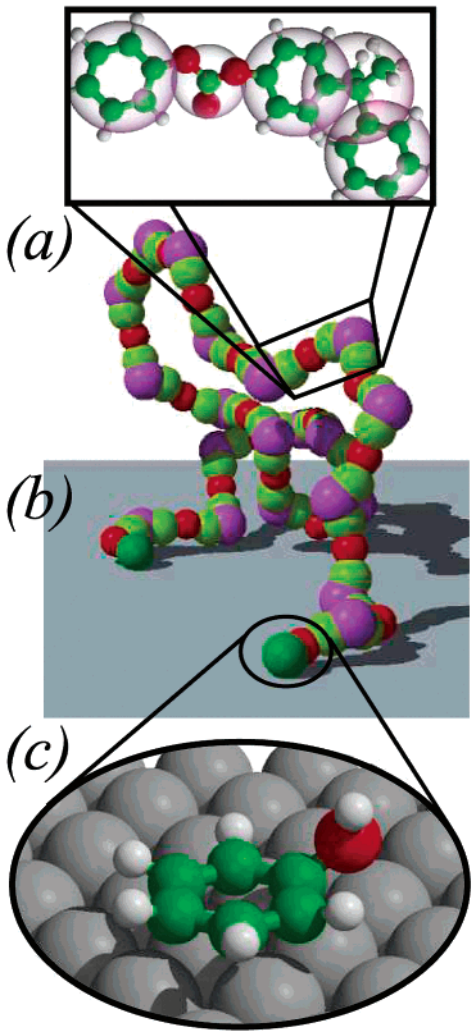

Figure 2. Pictorial representation of the multiscale model of BPA-PC on the (111) surface of nickel. Reprinted with permission from Delle Site, L.; Abrams, C. F.; Alavi, A.; Kremer, K. *Phys. Rev. Lett.* **2002**, *89*, 156103. Copyright 2002 by the American Physical Society.

containing different end groups next to a perfect metal surface. As a first example, we look at a Ni(111) surface; this and metal surfaces, in general, are of particular relevance for studies of surface properties as well as industrial processing. In recent publications, some of us reported the development of a multiscale technique specifically designed to simulate polymers next to metal surfaces and applied it to the case of phenolic end groups (see Figure 2).[1,2,10] This included an appropriate coupling of information from detailed ab initio calculations of small molecule/surface interactions (see Appendix and ref 35) into coarse-grained molecular-dynamics simulations of liquids of the much larger macromolecules. To faithfully represent the conformations near the surfaces, a dual scale simulation was developed, where the bond angles at the terminal carbonate group had to be included explicitly into the coarse-grained model. Within this calculation, it was shown that short BPA-PC chains having phenolic end groups strongly adsorb with the ends to the surface, leading to significantly modified conformations near the surface. In the present study, we extend this investigation to a number of commonly used end groups. For

(15) Schmid, F.; Muller, M. *Macromolecules* **1995**, *28*, 8639.
(16) Fleer, G. J.; Cohen Stuart, M. A.; Scheutjens, J. M. H. M.; Cosgrove, T.; Vincent, B. *Polymers at Interfaces*; Chapman & Hall: New York, 1998.
(17) Abrams, C. F.; Kremer, K. *J. Chem. Phys.* **2001**, *115*, 2776.
(18) Abrams, C. F.; Kremer, K. *J. Chem. Phys.* **2002**, *116*, 3162.
(19) Hahn, O.; Delle Site, L.; Kremer, K. *Macromol. Theory Simul.* **2001**, *10*, 288.
(20) Abrams, C. F.; Kremer, K. *Macromolecules* **2003**, *36*, 260.
(21) Morbitzer, L.; Grico, U. *Angew. Makromol. Chem.* **1988**, *162*, 87.
(22) Yee, A. F.; Smith, S. A. *Macromolecules* **1981**, *14*, 54.
(23) Schaefer, D.; Hansen, M.; Bümilich, B.; Spiess, H. W. *J. Non-Cryst. Solids* **1991**, *131−133*, 777.
(24) Floudas, G.; Higgins, J. S.; Meier, G.; Kremer, F.; Fisher, E. W. *Macromolecules* **1993**, *26*, 1676.
(25) Weigand, F.; Spiess, H. W. *Macromolecules* **1995**, *28*, 6361.
(26) Wimberger-Friedl, R.; Schoo, H. F. *Macromolecules* **1996**, *29*, 8871.
(27) Li, L.; Yee, A. F. *Macromolecules* **2002**, *35*, 425.
(28) Shih, J. H.; Chen, C. L. *Macromolecules* **1995**, *28*, 4509.
(29) Fan, C. F.; Tahir, C.; Shi, W. *Macromol. Theory Simul.* **1997**, *6*, 83.
(30) Tsai, S. F.; Lan, I. K.; Chen, C. L. *Comput. Theor. Polym. Sci.* **1998**, *8*, 283.
(31) Bendler, J. T. *Comput. Theor. Polym. Sci.* **1998**, *8*, 83.
(32) Ballone, P.; Montanari, B.; Jones, R. O. *J. Chem. Phys.* **1999**, *103*, 5387.
(33) Robyr, P.; Gan, Z.; Suter, U. W. *Macromolecules* **1998**, *31*, 6199.
(34) Utz, M.; Robyr, P.; Suter, U. W. *Macromolecules* **2000**, *33*, 6808.
(35) Delle Site, L.; Alavi, A.; Abrams, C. F. *Phys. Rev. B* **2003**, *67*, 193406.

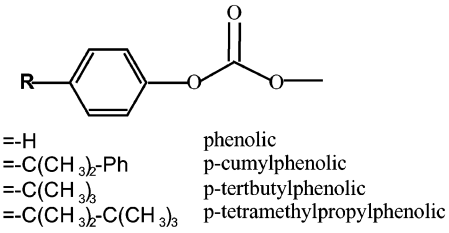

Figure 3. Four of the most technologically relevant chain terminations of BPA-PC.

comparison, we also include some of the previous results on the phenolic end groups.

II. Ab Initio Calculations for BPA-PC

Figure 3 shows four chain-end modifications of BPA-PC considered: (a) phenolic, (b) *p*-cumylphenolic, (c) *p-tert*-butylphenolic, and (d) *p*-tetramethylpropylphenolic. The case of a phenolic chain end[1,2,10] will be reported for comparison, and attention will be focused on modeling the interaction of the other three chain ends with the nickel surface. For internal monomers, the modeling procedure is the same as in previous work and will only briefly be reviewed in the next section. As underlined before, the reason for doing ab initio calculations is that for polymers interacting with a surface there could exist a situation where specific local interactions influence global properties. The approach we have chosen is to obtain information about molecular adsorption at the surface using an ab initio method and then to incorporate such information into a coarse-grained bead-spring model for the polymers. To do so, the chain is cut into comonomeric submolecules small enough to treat the interaction with the surface in detail for each of them. As illustrated in Figure 1 for BPA-PC, carbonic acid represents the carbonate group, propane represents the isopropylidene, and benzene (phenol) represents the phenylene. The molecule/surface ab initio study has to be performed in such a way that the submolecules mimic the behavior of a monomer or a chain end within a BPA-PC chain near the surface. To fulfill this requirement, we select those molecular orientations which are compatible with chain conformations at the surface. Next, we take the most representative (allowed) orientations and use them as a starting geometry for a BFGS geometry optimization at each high-symmetry site of the (111) nickel surface using the FEMD code[36−38] (see Appendix). Finally, the resulting optimized geometries are checked to see whether they are still compatible with the allowed chain conformations at the surface; for those which are compatible, adsorption energies are taken to estimate the strength of the interaction with the surface. Of course, for the chain ends, different additional orientations as compared to the inner fragments are to be considered.

For the chain ends specified above, we take advantage of the fact that each chain end considered can be divided into submolecules corresponding to those already treated in our previous work (see Figures 1 and 3). This means that additional ab initio calculations would not be required. However, for *p-tert*-butylphenol and *p*-tetramethylpropylphenol, a neopentane molecule (2-dimethyl-propane), $C(CH_3)_4$, is somewhat more appropriate but also more complex than a propane as a terminating molecule. For that reason, we performed some preliminary ab initio calculations for this molecule as well. We found its behavior near a nickel surface to be qualitatively and quantitatively equivalent to that of propane. We thus can refer to the results of propane for modeling the chain-end interaction with the surface. As anticipated in the previous sections, our multiscale modeling consists of an appropriate combination of ab initio molecule/surface results and polymer allowed conformations at the surface, which increase in the case of chain ends. In the next sections, we will give a general description of the ab initio procedure used and the results obtained. For each specific chain end, we will then describe how these ab initio results are incorporated into the coarse-grained model with the surface.

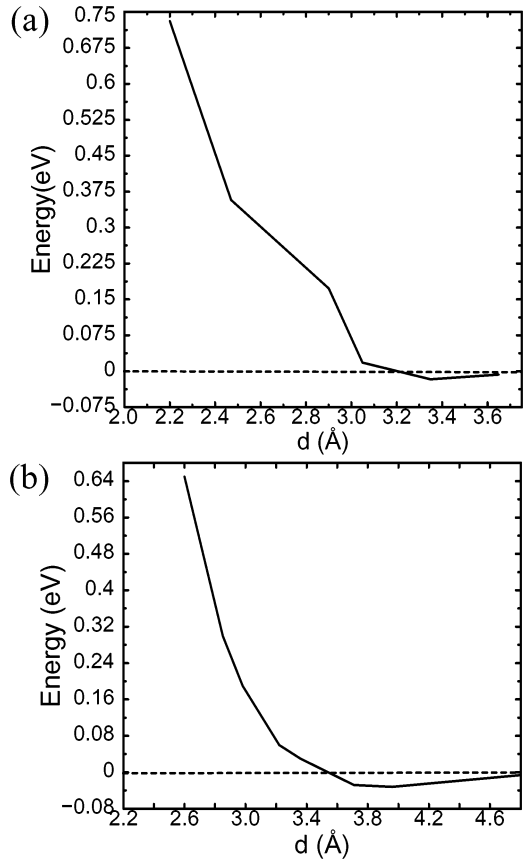

Figure 4. Adsorption energy of carbonic acid (a) and propane (b) as a function of the respective carbon distance from the surface. Initially an optimal geometry is obtained by allowing all of the degrees of freedom to relax; next the molecule is moved toward (or away from) the surface in adiabatic steps. At each step, the *z*-coordinate of the central carbon atom is kept fixed and the remaining degrees of freedom are relaxed; in this way, a *z*-dependent adsorption energy is obtained.

A. Carbonic Acid and Propane: Ab Initio Results. Here, we briefly report the results obtained from the ab initio calculations of carbonic acid and propane on a (111) nickel surface. More details are given in the Appendix. Figure 4 shows the adsorption energy of carbonic acid and propane as a function of the distance from the surface. The relevant feature to emerge from this study is that both molecules experience the surface as a (uniform) hard wall with a characteristic minimal distance of about 3.2 Å. Below this distance, the molecules feel a strongly

(36) Hutter, J.; Alavi, A.; Deutsch, T.; Bernasconi, M.; Goedecker, S.; Marx, D.; Tuckerman, M.; Parrinello, M. *CPMD v. 3.4.1*; Max-Planck-Institut für Festkörperforschung and IBM Zurich Research Laboratory, 1995−1999.
(37) Alavi, A.; Kohanoff, J.; Parrinello, M.; Frenkel, D. *Phys. Rev. Lett.* **1994**, *73*, 2599.
(38) Alavi, A. In *Monte Carlo and Molecular Dynamics of Condensed Matter Systems*; Binder, K., Ciccotti, G., Eds.; Italian Physical Society: Bologna, 1996.

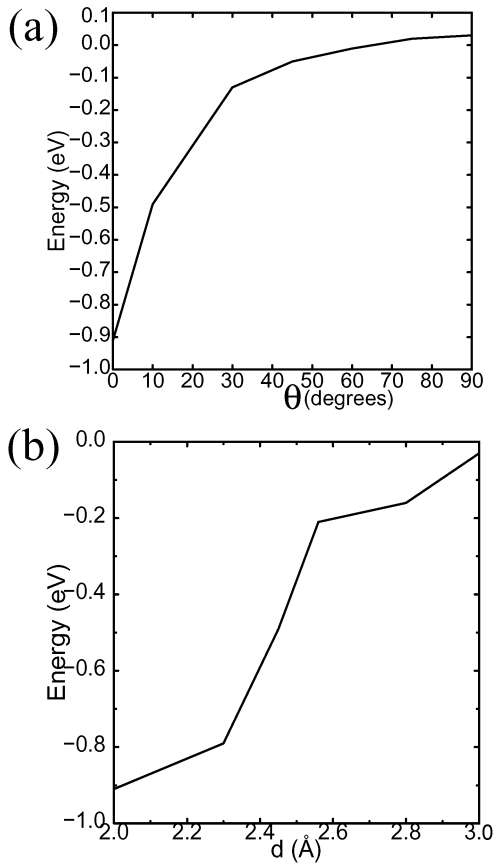

Figure 5. Adsorption energy of phenol at the bridge site as a function of the inclination of the carbonic ring (a), at a distance of 2.0 Å, and as a function of the distance from the surface (b). Plot (a) is taken from ref 2, where details about the calculation can be found, and is reprinted with permission from Abrams, C. F.; Delle Site, L.; Kremer, K. *Phys. Rev. E* **2003**, *67*, 021807. Copyright 2003 by the American Physical Society. Plot (b) had been obtained by moving adiabatically away from the optimal adsorption distance. During the optimization, the *z*-coordinate of the carbons was kept fixed. The same calculations with fewer data were performed also for benzene and show a qualitative behavior similar to that of phenol. Notice that in both cases the adsorption potential is short ranged.

increasing repulsion as the distance decreases, taking the thermal energy k_BT in our simulations as a reference. Discussions about the limitations of the ab initio approach in describing dispersion forces can be found in refs 2, 10, and 35; in any case, we should underline that because we work at the typical process temperature of ∼570 K, they do not play an important role because they are too small (of the order of k_BT, where $k_BT \approx 0.05$ eV).

B. Benzene and Phenol: Ab Initio Results. Benzene and phenol show a strong adsorption at each high-symmetry site of the (111) nickel surface with the exception of the atop site. For benzene, depending on surface site and molecular orientation, the adsorption energy is in the range 0.7−1.0 eV, while for phenol it is in the range of 0.64−0.91 eV. In both cases, the carbon ring lies parallel to the surface at an equilibrium distance of about 2.0 Å. The adsorption energy reduces at the atop site. However, this site is statistically not relevant because the diffusion barrier is low enough to allow the molecule to migrate toward a more stable site (as test calculations indicate). In view of these results, one can conclude that in general isolated benzene or phenol strongly binds lying flat on the surface, at an average equilibrium distance of 2.0 Å. These results are extensively discussed in ref 35. However, understanding the

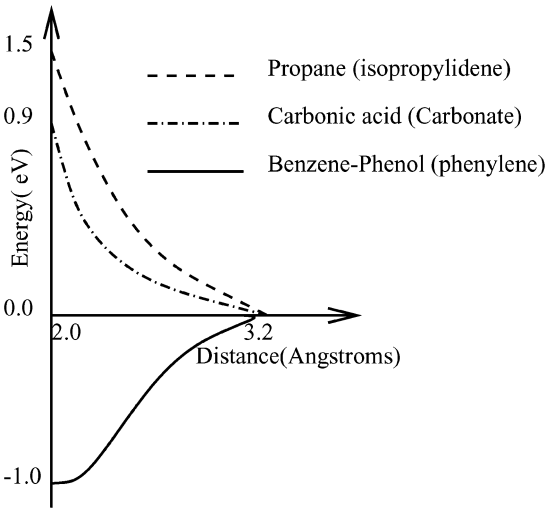

Figure 6. Schematic summary of the ab initio results obtained. This scheme suggests that it is unlikely that an internal phenylene will find an optimal adsorption distance (configuration) due to the strong repulsion experienced by the two neighboring beads to which the phenylene is topologically connected.

optimal adsorption conformation of benzene and phenol on the surface is not sufficient for our modeling procedure. Figure 5 shows the adsorption energy of phenol as a function of inclination (a) and distance (b) from the surface at the most favorable high symmetry site (bridge). For benzene, within a 5% difference, it is the same. For this reason, we will refer to phenol potentials in the next sections when modeling the phenylene interaction (for both internal monomer and chain ends) with the surface. The adsorption potential is inclination dependent and very short ranged. This implies that as soon as we move away from the optimal configuration, the strength of the adsorption strongly decreases. We now use this information to construct an ab initio-based model for the interaction Ni/BPA-PC monomer (and chain ends).

C. Ab Initio Modeling of Internal Monomers. Figure 6 shows a schematic summary of the ab initio results of the previous sections, which also helps to clarify the interaction of internal monomers with the surface. In fact, one can conclude that carbonic acid and propane see the surface as a hard repulsive wall. Below distances of 3.2 Å from the surface, they experience significant repulsion which strongly increases as distance decreases. Consequently, these molecules explore shorter distances from the surface at vanishing probabilities. Phenol and benzene, which show strong adsorption in isolation, are sterically forbidden to adsorb when incorporated into a BPA-PC monomer. In fact, due to constraints induced by their neighboring carbonate and isopropylidene groups and to the short range nature (as a function either of distance or of inclination) of phenol (benzene) adsorption, it is not possible that phenylene can reach an optimal adsorption conformation. In conclusion, for internal beads, we can model the interaction with the surface by a purely repulsive potential. For chain ends, this is different.

D. Ab Initio Modeling of Chain Ends. Chain ends can explore additional conformations that can lead to adsorption. This indeed is the case for phenolic chain ends. There the optimal adsorption conformation for phenol or benzene at the BPA-PC chain end is possible. For the other chain ends considered in this study, the situation is different. They are represented by a sequence of single submolecules, with conflict-

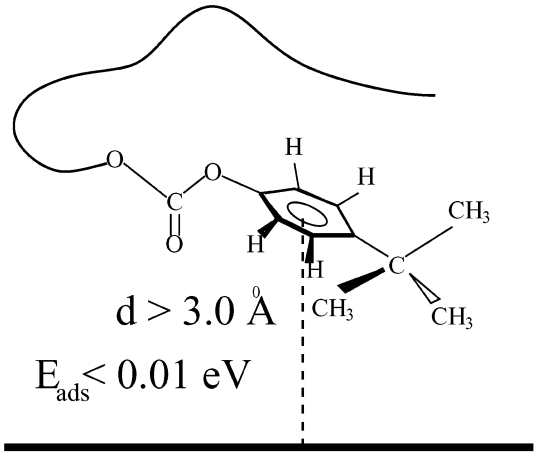

Figure 7. An example of a possible chain-end conformation at the surface. Because the propane (or neopentane) shows a strong repulsive behavior for distances below 3.2 Å and the benzene-like submolecule does not reach an optimal distance for its adsorption (beyond 3.0 Å, the attraction vanishes), the chain end in such a conformation (or similar) experiences the surface as a purely repulsive hard wall.

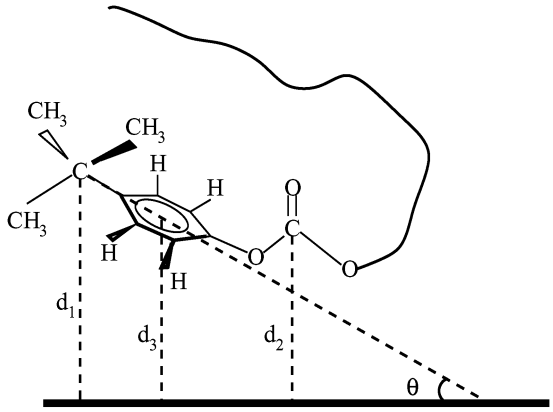

Figure 8. An example of another possible chain-end conformation at the surface. In this case, the benzene-like submolecule reaches distances (d_3) and inclinations (θ) which are characterized by an attractive interaction in isolation (i.e., for the isolated benzene or phenol). To estimate the total interaction energy of the chain end, we have to consider the other variables of the problem, the propane and carbonic acid potential for a range of distances, d_1 for propane and d_2 for carbonic acid, corresponding to the (θ, d_3) which gives attraction. It is important to notice that, because of the topological connectivity, one needs to specify only d_1 and d_2; θ and d_3 are automatically specified. Calculations show that, for the whole possible range of attractive configurations (θ, d_3), the total energy of the chain end is always repulsive; thus the BPA-PC melt with *p-tert*-butylphenolic chain ends is characterized uniquely by entropic interactions at the surface.

ing attraction and repulsion, respectively. In those cases, a detailed statistical analysis of the allowed conformations is carried out case by case. For each allowed conformation, by using the ab initio potentials shown before, we estimate whether chain ends adsorb strongly.

In performing an ab initio-based modeling of chain ends composed of more than one submolecule, we have to properly combine ab initio results for single submolecules (shown in the previous sections) with statistical conformations of the whole unit which represents the chain end. For this purpose, let us define the following potentials: $U_{carb}(z)$ corresponding to the carbonic acid adsorption potential of Figure 4a, $U_{prop}(z)$ corresponding to the propane adsorption potential of Figure 4b, $U_{phenol}(\theta)$ corresponding to the phenol adsorption potential of Figure 5a, and $U_{phenol}(z)$ corresponding to the phenol adsorption potential of Figure 5b. To take into account the dependence of the adsorption potential for phenol as a function of inclination and distance simultaneously, we use an approximation made previously:[2]

$$U_{phenol}(z,\theta) = \frac{U_{phenol}(\theta) \times U_{phenol}(z)}{U_{phenol}(\theta_0, z_0)} \qquad (2.1)$$

where $U_{phenol}(\theta_0, z_0)$ is the adsorption energy (0.91 eV) at the optimal configuration ($\theta_0 = 0.0$; $z_0 = 2.0$ Å). As can be easily checked, this ansatz gives the correct behavior in the limiting case of one variable fixed at its optimal value, for example, for $\theta = 0.0$, $U_{phenol}(z,\theta = 0.0) = U_{phenol}(z)$ and vice versa. At this stage, from the point of view of potentials, we have enough information to estimate the strength of the interaction of each chain end with the surface. The next step is to select those conformations of closest approach of benzene to the surface which do not violate any steric hindrance. In the following section, we will proceed with the modeling for each specific chain.

E. *p-tert*-Butylphenolic Chain End. Figures 7 and 8 show how the benzene in the *p-tert*-butylphenolic chain end can approach the surface. In the first case, the conformation is clearly nonattractive on the basis of the considerations made in the previous sections. In the second case, phenol (benzene) might reach distances and inclinations which correspond to the attractive regime of $U_{phenol}(z,\theta)$ in isolation. To determine whether the chain end (as a whole) is attracted by the surface, we consider (for (d_3,θ) with attractive $U_{phenol}(z,\theta)$) the distance-dependent potential of the other two submolecules for the corresponding distances d_1, d_2, in simple terms:

$$U_{chainend}(d_1, d_2,\theta) = U_{prop}(d_1) + U_{carb}(d_2) + U_{phenol}(d_3,\theta) \qquad (2.2)$$

where $U_{chainend}(d_1, d_2,\theta)$ is the total chain-end potential for given distances of submolecules and carbon ring inclination. Because the chemical bonds are almost rigid, we need only three parameters (d_1,d_2,θ), and the fourth (d_3) is automatically determined. In principle, one should also consider possible lateral rotations of the phenylene around the axis defined by the $C_{isopropylidene}-O_{carbonate}$; however, the rotational barrier is of the order of the thermal energy of the melt, and in a good approximation we can neglect it. Test calculations of benzene and phenol show that lateral rotations reduce the surface interaction. Our calculations show that $U_{chainend}(d_1,d_2,\theta)$ is always positive (repulsive). Thus, the potential of the chain end is always repulsive, and we conclude that the *p-tert*-butylphenolic chain end sees the surface as a purely repulsive hard wall. This is the relevant information introduced into the coarse-grained model.

F. *p*-Tetramethylpropylphenolic Chain End. For this chain end, from an ab initio point of view, the considerations for *p-tert*-butylphenolic hold as well. In fact, the only difference is that the terminating molecule is larger than propane or neopentane but with a similar repulsive behavior. The equilibrium distance from the surface of the isolated molecule is slightly larger, due to the larger molecular size which will be properly considered in the coarse-grained model. In conclusion, on the basis of the ab initio estimate, the *p*-tetramethylpropylphenolic chain end, as the *p-tert*-butylphenolic, sees the surface as a purely repulsive hard wall.

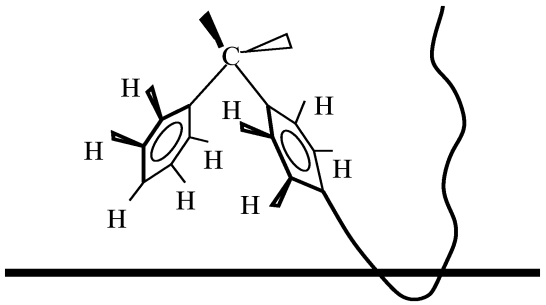

Figure 9. An example of a conformation for the *p*-cumylphenolic chain end which is not allowed. To have inclinations and distances for which $U_{phenol}(z,\theta)$ shows relevant attraction values, due to the rigidity of the polymer connectivity, part of the chain should penetrate the surface.

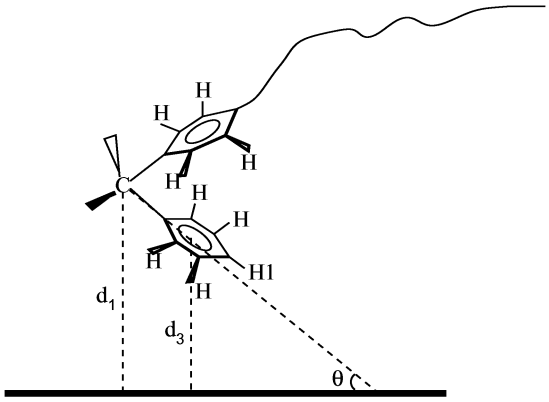

Figure 10. An example of a conformation for the *p*-cumylphenolic which leads to an attractive behavior.

G. *p*-Cumylphenolic Chain End. Again, we follow the same procedure as above to search for possible attraction to the surface. Figure 9 shows, for the *p*-cumylphenolic chain end, an example of a configuration which is not allowed. Due to the polymer rigidity and connectivity and the rigid tetrahedral structure of the chain ends, distances of the benzene closest to the end, which would allow for attraction, require parts of the chain to penetrate the surface. Other configurations such as those where the isopropylidene points at the surface ("V" conformation) are purely repulsive because $U_{propane}$ dominates. To experience attractive values for $U_{phenol}(z,\theta)$, the isopropylidene has to approach the surface so closely that its repulsion would be much larger than the maximum attractive energy $U_{phenol}(z,\theta)$ of each neighboring phenylene combined. The remaining conformations are those shown in Figure 10. In this case, we found a range of parameters d_1, d_3,θ for which some attraction of the chain end can occur. In considering such conformations, one again should keep in mind that any rotation of the phenylene along the C−H_1 axis can be neglected. If this would not be possible, then one should have considered all of the possible "rotated" configurations, and the attractive conformations would be statistically of low probability. Also, a different coarse-grained bead-spring model would be needed. Figure 11 shows the attractive energy U_a of the *p*-cumylphenolic chain end as a function of the carbon ring inclination (θ) at representative isopropylidene distances (d_1) (remember that $d_3 = f(d_1,\theta)$). The attractive potential is defined positive, and the repulsive energy is not represented; U_a is measured in k_BT where the temperature is the typical temperature for a melt processing of BPA-PC (570 K). As one can see, there is a restricted range of θ and d_3 for which an attractive potential arises and the maximum value

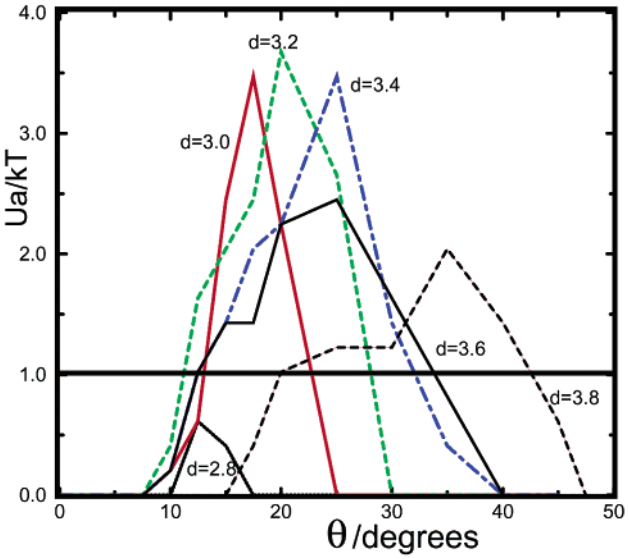

Figure 11. The attractive energy U_a as a function of the carbon ring inclination (θ) at representative isopropylidene distances (d_1) for conformations shown in the previous figure. U_a is defined positive, and repulsion (in this case defined negative) is not shown. The energy is measured in k_BT, $T = 570$ K, to make a direct comparison directly with the energy scale of the melt. As it is possible to see, the range of isopropylidene distances, d_1, is extremely small (3.0−3.8 Å), and the range of θ is within 15−40°, which is a relatively small range; moreover, the maximum attraction energy is about 3.5 k_BT, which is, on a statistical average, within the thermal fluctuations of the system.

reachable (∼3.5 k_BT) is, anyway, within the thermal fluctuations of the system. On the basis of these calculations, one can infer that this attractive behavior can lead to an "energetic perturbation" of the entropy dominated regime near the surface. In proceeding toward a coarse-grained model, we will use these results and in particular those of Figure 11 to model the behavior of the *p*-cumylphenolic chain end at the surface.

III. Coarse-Grained Model

In this section, we describe the coarse-grained model for a BPA-PC melt near a metal surface. Because the modeling of the inter- and intrachain potentials was presented elsewhere,[20] attention will be mostly focused on the interaction of internal monomers and chain end with the surface.

A. Inter- and Intrachain Interactions. We employ the model used in our previous work, where it is discussed in detail.[20] Briefly, each repeat unit (see Figure 1) is replaced by four beads that correspond to the basic molecular units: isopropylidene, carbonate, and the two linking phenylenes. Intrachain potentials involving the coarse-grained variables were derived from the Boltzmann factors of single chain distributions relative to those variables. All beads interact with each other via a spherical excluded volume potential of the form of a truncated and shifted repulsive 12-6 Lennard-Jones pair potential. The size of the isopropylidene bead is 5.19 Å, of the carbonate is 3.49 Å [note that in refs 2, 20, a misprint occurred, and a carbonate size of 4.49 Å instead of the correct value of 3.49 Å was given], and of the phenylene is 4.67 Å, respectively.

B. Interaction Potential of Internal Monomers with the Surface. The interaction of internal beads with the nickel surface was also studied in our previous work.[1,2] The systems consist of melts with a slit pore of width L with walls normal to the z-direction and periodic boundary conditions in x and y. All

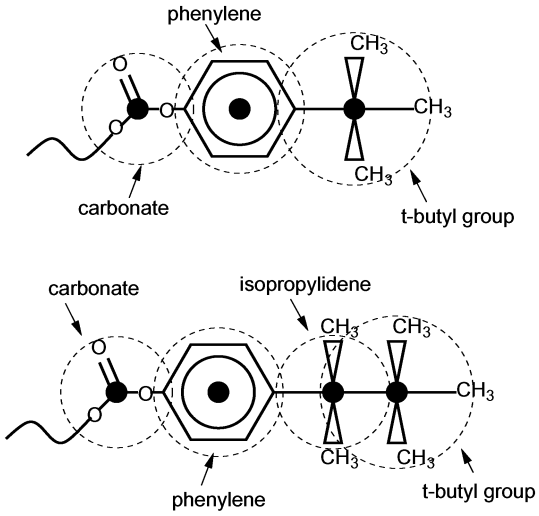

Figure 12. The coarse-grained scheme for the *p-tert*-butylphenolic and *p*-tetramethylpropylphenolic chain ends. A new bead type is introduced to properly take into account the excluded volume of the chain end. The *tert*-butyl part is characterized by a volume which is larger than the isopropylidene to properly take into account the larger molecular size.

internal beads interact with the walls via a one-dimensional 10-4 repulsive potential:

$$U_{w,rep}(z) = U_{10-4}(z) + U_{10-4}(L_z - z) \qquad (3.1)$$

$$U_{10-4}(z) = \begin{cases} 2\pi\epsilon_w \sigma_w^2 \left[\frac{2}{5}\left(\frac{\sigma_w}{z}\right)^{10} - \left(\frac{\sigma_w}{z}\right)^4 + \frac{3}{5}\right] & ; z < \sigma_w \\ 0 & ; z \geq \sigma_w \end{cases} \qquad (3.2)$$

with z being the distance from the wall. σ_w for each type of bead was taken from ab initio calculations (in this case, σ_w = 3.55 Å for isopropylidene and carbonate). ϵ_w and σ_w were chosen so that each bead experiences 1 k_BT of repulsive energy at a distance of 0.9 σ_w. This prevents any internal phenylene from adsorbing to the flat surface. For chain ends, the situation is different and will be treated in detail below.

C. *p-tert*-Butylphenolic and *p*-Tetramethylpropylphenolic Chain Ends at the Surface. For these two types of chain ends, according to the ab initio modeling presented above, a potential similar to that used for internal monomers in eq 3.1 is appropriate. Each single bead experiences just a repulsive interaction below a given distance from the surface. The difference for internal monomers is given by the fact that in this case a new bead type corresponding to the *tert*-butyl has been introduced (see Figure 12). Intramolecular potentials of the new bead are identical to those of isopropylidene; the radius of the excluded volume corresponds to 1.5 times that of isopropylidene.

D. *p*-Cumylphenolic Chain End. Consistent with the ab initio estimate of the attractive potential for this chain end shown in Figure 11, a potential has been introduced into the coarse-grained model of the chain end. This interaction is constructed as a sum of two repulsive potentials for isopropylidene and phenyl and one attractive potential for an additional interaction site located in the middle point of the bond between the two chain-end beads (see Figure 13). This potential takes the form:

$$U_a(z) = U_{10-4}^{\text{isopropylidene}}(z) + U_{10-4}^{\text{phenyl}}(z) + U_{mp}(z) \qquad (3.3)$$

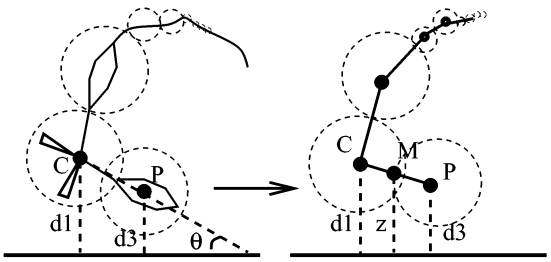

Figure 13. The coarse-grained scheme for the *p*-cumylphenolic chain end. The dependence from d_1, d_3, θ is described by introducing an additional interaction site M located at the middle point of the C−P bonding segment.

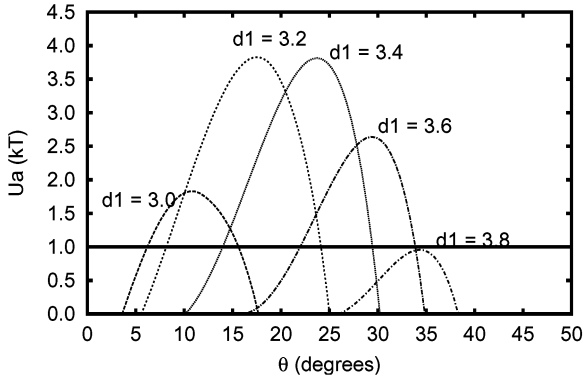

Figure 14. The coarse-grained potential obtained by modeling the interaction with the surface suggested by the previous figure and based on the ab initio modeling. As it is possible to see, the coarse-grained potential describes quite well the qualitative and, within the resolution of the model, the quantitative ab initio data.

$U_{10-4}^{\text{isopropylidene}}(z)$ and $U_{10-4}^{\text{phenyl}}(z)$ have the same form shown in eq 3.1; in this case, σ_w takes the value of 3.6 Å for isopropylidene and 2.8 Å for phenyl, while (σ_w, ϵ_w) lead to an energy of 1 k_BT at a distance of 3.2 Å from the surface for isopropylidene and 2.2 Å for phenyl. The potential of the additional interaction site located at the middle point has the form:

$$U_{mp}(z) = \begin{cases} 2\pi\epsilon_w z_0^2 \left[\frac{2}{5}\left(\frac{z_0}{z}\right)^{10} - \left(\frac{z_0}{z}\right)^4 + \frac{3}{5}\right] - \epsilon_{attr} & ; z < z_0 \\ \frac{1}{2}\epsilon_{attr} \cdot \left[\cos\left(\pi\frac{z_c - z}{z_c - z_0}\right) - 1\right] & ; z_0 \leq z < z_c \\ 0 & ; z \geq z_0 \end{cases} \qquad (3.4)$$

where z_0 is the distance of maximum effective attraction (∼2.7 Å); z_c corresponds to the distance cutoff, 3.2 Å; and ϵ_{attr} is the well depth of 5.5 k_BT. Figure 14 shows the potential of eq 3.3. As compared to Figure 11, the potentials in Figure 14 mimic the behavior described by the ab initio modeling in a rather reasonable way. The essence is to include the weak attraction as well as roughly the angular dependence, suggested by the ab initio estimate, to a good approximation into the coarse-grained model. Due to the accuracy of the model, small differences between 0.25−0.50 Å, 5−10°, and 0.5−0.7 k_BT cannot be resolved.

E. Simulation Details. Molecular dynamics simulations were performed in the NVT ensemble for melts of BPA-PC, characterized by different chain ends, in contact with a nickel surface. The temperature of the system was set to 570 K, and the conditions of the simulation along with the procedure to generate initial melt configurations were identical to those of

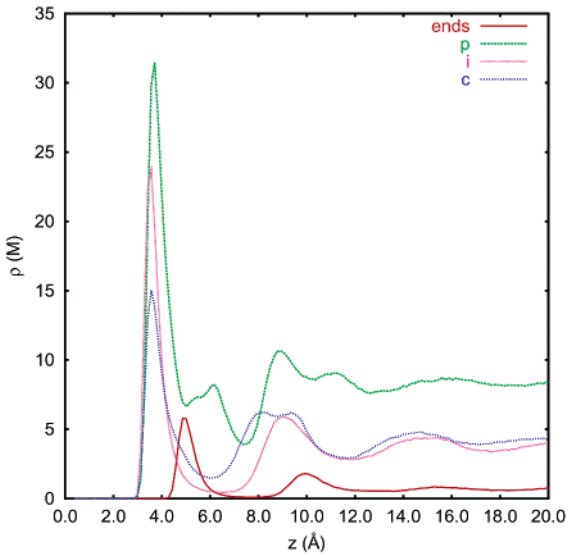

Figure 15. Bead depth profiles (number density versus distance from surface) of coarse-grained beads for the melt with *p*-tertbutylphenolic chain ends. Mirror image symmetry about the center line is applied. Shown are the profiles of end *tert*-butyls (ends), phenylenes (p), isopropylidenes (i), and carbonates (c). As expected, the density of chain ends near the surface is very low, while the density of internal beads is rather high. Little layering in the density profiles is observed.

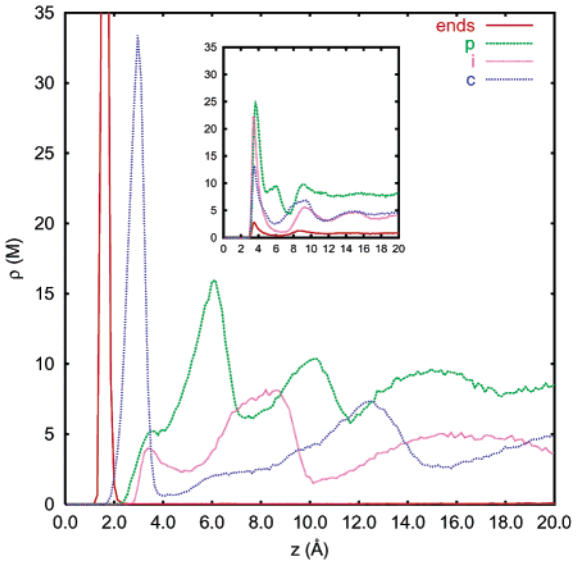

Figure 16. Bead depth profiles of coarse-grained beads obtained from the results of ref 2 for a melt with phenolic chain ends. Shown are the profiles of end phenoxy (ends), internal phenylenes (p), isopropylidenes (i), and carbonates (c). The inset shows the corresponding profiles in the absence of attractive potential for the phenolic end groups. In the presence of adsorption, chain ends are strongly localized at the surface, while in its absence, the density of chain ends near the surface is very low, and that of internal beads is rather high.

refs 1, 2. In such a procedure, chains are randomly placed in a box and grown according to the bond length and bond angle probabilities (for details, see ref 8), and then bead−bead overlaps are removed in a "push-off" integration[17] where particles interact via a radially shifted Weeks−Chandler−Anderson repulsive particle−particle pair potential with a radial shift term that decays linearly to zero over the duration of this push-off stage. In a second phase, wall potentials are applied, with the origins first at a distance containing all of the beads in the system and then brought them closer until the appropriate bulk density has been reached. The samples consist of 240 chains of 10 repeat units. For the *p*-cumylphenolic chain end, additional simulations were also carried out for a melt of 240 chains of five repeat units, but at the same density. Equilibration was assumed after the chains have moved in average a distance equivalent to their radius of gyration. The system density was fixed at 1.05 g/cc, the experimental system density at 570 K. The box dimensions (x, y, z) are set to be consistent with previous work;[2] that is, x and y are set to 98.0 and 95.8 Å, respectively, which correspond to a (111) hexagonal lattice with 36 orthohexagonal unit cells in the x direction and 22 in the y direction. The z dimension is 110.3 Å for the phenol-ended chains, for the *p*-tertbutylphenolic case it is 116.1 Å, while for the *p*-tetramethylpropylphenolic and *p*-cumylphenolic cases it is 121.3 Å, for chains with 10 repeat units. Only for the test case of chains with 5 repeat units and *p*-cumylphenolic end chains is z 69.2 Å. In terms of LJ-units σ, often quoted in other publications, this gives $1\sigma = 4.41$ Å.

IV. Results

Results from the simulation of the melts with the *p*-alkylphenolic chain ends, *p*-tertbutylphenolic and *p*-tetramethylpropylphenolic, are shown in Figure 15. The number density of beads is displayed as a function of distance from the walls, z. These plots show that a certain amount of internal beads is localized near the Ni surface, while the density of chain ends in the same region is very small. This is not a surprising result, provided the purely repulsive interaction of the chain ends with the surface, which is a hard wall, and their bulky size. That behavior is clearly different from that of a melt of phenol-ended BPA-PC chains,[2] which is summarized in Figure 16. In that case, phenolic chain ends strongly adsorb on Ni, and as a consequence energy plays a crucial role for the properties close to the wall. This results in a significant localization of chain ends at the surface and most noticeably in a strong layering of the density profiles. This layering extends out to a depth of about the average radius of gyration (around 20.5 Å) of the relatively short chains considered. In contrast, for melts with *p*-alkylphenolic chain ends, any trace of structure of the profiles already vanishes at a distance of around 10 Å from the wall. In this case, conformational entropy rules the local bead packing of the melt close to the wall.

To obtain a better picture of the effect of the specific size of the nonadsorbing chain end on the morphology close to the wall, the previous results have been compared to those obtained for melts with phenolic and *p*-cumylphenolic ends in the absence of any attractive potential. Identical bead depth profiles are obtained for both systems (see inset in Figure 16 for the profiles of the phenol-terminated chains), that are also quite similar to those of the nonadsorbing *p*-alkylphenolic groups. Differences between the different profiles are only quantitative, referring mostly to the density in the region close to the walls up to the ends themselves. Thus, the relatively large size of the *p*-alkylphenolic chain ends hinders their localization at the surfaces, so the density of internal beads becomes higher than that for the phenolic-ended chains, where the smaller chain end can more closely approach the walls. It is also interesting to note that the density of both *p*-alkylphenolic chain ends close to the wall is the same, even though the *p*-tetramethylpropylphenolic group is bigger than the *p*-tertbutylphenolic, and the density of internal beads at the surface is slightly lower due to

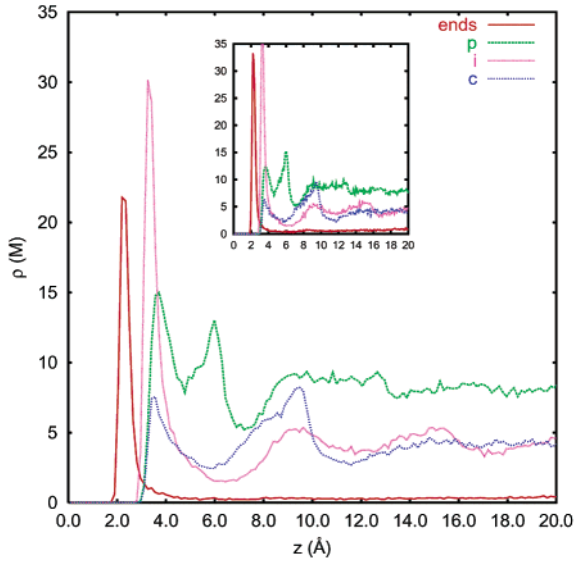

Figure 17. Bead depth profiles of coarse-grained beads for the melt with 10 repeat units per chain and with *p*-cumylphenolic chain ends. Shown are the profiles for end phenyl (ends), internal phenylenes (p), isopropylidenes (i), and carbonates (c). The inset shows the corresponding profiles for $N = 5$ repeat units.

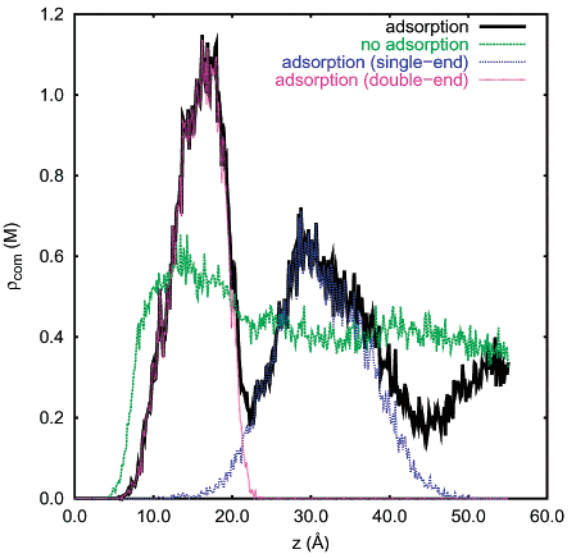

Figure 18. Chain center-of-mass depth profiles for the melts with phenolic chain ends, with and without attractive potential. Division into populations of chains which adsorb one or both ends on the surface are also shown for the case with attractive potential. Data for the melt with adsorbing chain ends are obtained from ref 2. With adsorption, two layers are clearly observed, corresponding to a layer containing chains with both ends adsorbed on the surface, and another layer formed by chains with a single end adsorbed. Each layer extends about one radius of gyration, so the layering structure extends until two radius of gyration from the walls. Without adsorption, no clear layering is observed.

size effects. One should however keep in mind that such subtle differences might be reduced when atomistic details are reintroduced.

For *p*-cumylphenolic chain ends, the situation is somewhat different, as Figure 17 displays. It can be seen that there is a certain amount of chain ends localized at the surface, as a result of the weak attraction to Ni. However, in contrast to phenol-ended chains, this adsorption seems to have little effect on the structure of the melt, because layering of the density profiles is much weaker. Actually, after a distance of 10 Å from the wall, the profiles are almost the same as for the nonadsorbing chain ends. These results suggest that the weak adsorption of the *p*-cumylphenolic chain end can be viewed only as a local perturbation, while conformational entropy plays again the most important role regarding the behavior of the system. Because this might be stronger for short chains, the influence of chain length for this specific case is checked, and a melt of chains with five repeat units is considered. The resulting bead depth profiles (see inset Figure 17) show a density of adsorbed chain ends larger than that for the longer chains, but still quite lower than that obtained for phenolic chain ends. Again, the density profiles are only weakly altered on a short scale corresponding roughly to the monomer size.

The different surface structure of the present melts of rather short chains is best illustrated by the center-of-mass density profiles as a function of the distance from the walls, that are displayed in Figures 18−20. For the melt with phenol chain ends (see Figure 18), two distinct layers are clearly observed, corresponding to a layer constituted by chains with the two ends adsorbed on the surface and another with chains with single-adsorbed ends.[2] In the absence of any adsorption, no layering is observed, as for the other chain ends. Even for the *p*-cumylphenolic end (see Figure 19), which experiences some attraction, this effect is very weak with a small tendency toward a stronger layering for the small 5-mers.

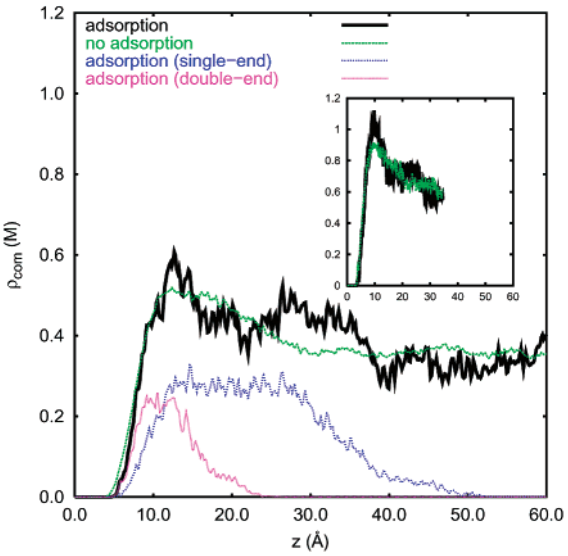

Figure 19. Chain center-of-mass depth profiles for the melts with *p*-cumylphenolic end groups, with and without attractive potential. The division into populations of chains, which adsorb one or both ends onto the surface, is also shown for the case with attractive potential. The inset, in addition, gives results for melts with 5 repeat units per chain.

V. Discussion

Our calculations show that chain-end modifications can lead to significantly altered melt morphologies close to the surface. Polycarbonate is composed of submonomers, which alternately are strongly attracted (benzene rings) and repelled (carbonate and isopropylidene) by the surface. As shown before, the specific chain structure prevents the internal benzene rings from close proximity to the surface and thus strong adsorption. Therefore, any specific interaction of BPA-PC with the Ni-(111) surface is due to different chain ends. Their specific (non)adsorption

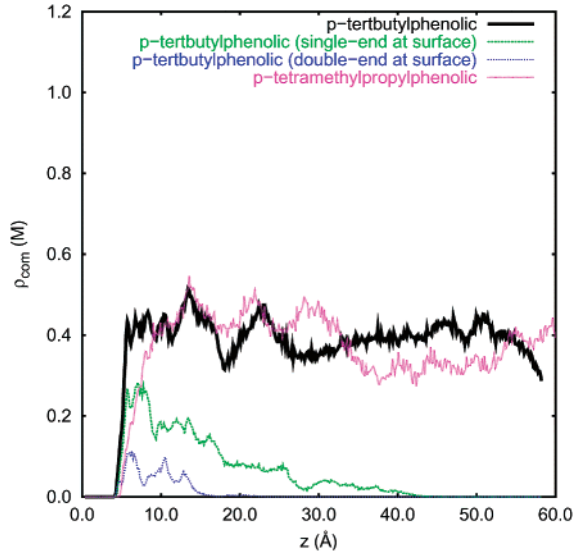

Figure 20. Chain center-of-mass depth profiles for the melts with *p*-tertbutylphenolic and *p*-tetramethylpropylphenolic chain ends. For the *p*-tertbutylphenolic ends, division into populations with one or both ends in contact with the surface (without energetic adsorption) is also shown.

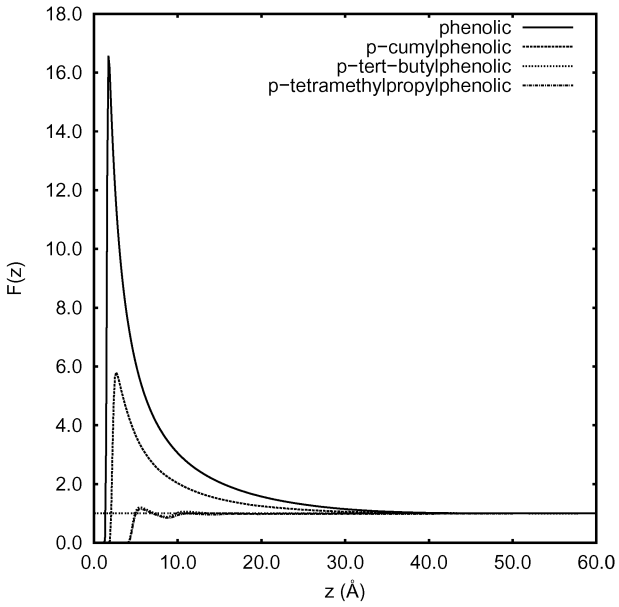

Figure 21. The plot shows the function $F(z_0) = (1/z_0 - 2.0)\int_{2.0}^{z_0}\rho_{end}(z)\,dz$ for the case of phenolic (strong adsorption), *p*-cumylphenolic (weak adsorption), *p*-*tert*-butylphenolic, and *p*-tetramethylpropylphenolic (no attraction).

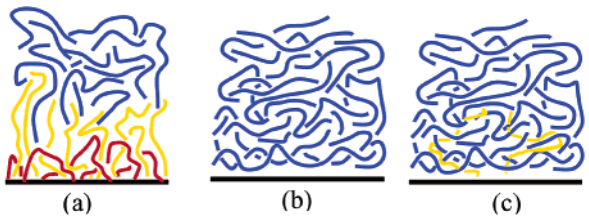

Figure 22. Three different situations occurring at the surface for the different chain-end melts. In the case of phenolic chain ends (a), a relevant number of chains is attached to the surface with both ends (red) or only one end with the rest of the chain pointing into the bulk (yellow). For the *p*-alkylphenolic chain ends (b), only conformational entropy governs the morphology at the surface. For the *p*-cumylphenolic chains ends (c), conformational entropy still governs properties at the surface, while few chain ends are weakly attached to the surface.

leads to pronounced effects, because the chains are relatively short. In the case of an effectively purely repulsive wall (*p*-alkylphenolic chain ends), the properties are dominated by the entropy of local packing. Although this is chemistry specific (or model specific if one deals with highly simplified models[20]), there are no strong chain length effects to be expected. The actual size of the ends supports even a tendency to locate them not directly at the surface. This is different for the case of strong adsorption of the chain ends (phenolic end). As was shown in earlier publications,[2,35] this leads to a significantly altered melt structure close to the surface. The surface is rather densely covered with chain ends. To accommodate for this, many chains are linked with both ends to the surface and consequently occupy a significant amount of available space in this region. Other chains, which have only one end at the surface, have, for pure packing reasons, to be somewhat stretched. However, we certainly are still far away from a true brush structure. Chains with no end linked to the surface are expelled from the immediate surface regime, leading to a characteristic rather strong segregation in the probability distribution of the chain centers of gravity, depending on whether they are lined with two, one, or no end to the surface (Figure 18). That this is a direct consequence of the chain-end adsorption is illustrated by the comparison to the repulsive hard wall results for the otherwise identical model. An interesting situation is found for the *p*-cumylphenolic chain ends in Figure 19, between the two extremes (phenol in Figure 18 and *p*-alkylphenolic ends in Figure 20). While the other two cases are either clearly energy or entropy dominated, the weak adsorption introduces slightly perturbed surface layers. However, the adsorption is too weak to significantly disturb the surface packing. Our findings are best summarized in two figures. Figure 21 shows the integrated average density of chain ends. The strong adsorption is clearly indicated by an enormous overshoot, while the repulsive wall introduces some very weak layering somewhat remote from the wall. The *p*-cumylphenolic chain end shows no signs of layering; however, it is still a weak overshoot as compared to phenolic ends, while the others even display a depletion of ends close to the surface. In a different way, one can cast the resulting morphologies into a rather simple cartoon, depicted in Figure 22.

VI. Conclusions

The above study was performed for short chains only, partly due to still rather significant computational demands. For strongly sticking chain ends, one certainly expects severe finite size effects, which eventually would prevent a strong binding of very long chains. However, all commercial and many experimental polymer samples are rather polydisperse, containing a large amount of shorter chains. Those shorter chains prefer to aggregate close to the surface, because their global conformation is weakly altered by the presence of the surface, if at all. Thus, our results are relevant for the specific case of the different typical end groups of BPA-PC close to a transition metal (Ni) surface. Depending on the purpose, the strong binding of the phenolic end group provides a rather efficient coating/contamination of the metal.

However, from the methodology as well as the physical effects studied, the present case can serve as just a specific example. By a combination of ab initio calculations together

with appropriately parametrized coarse-grained models of polymer−surface morphologies, which result from local chemistry, specific and global generic polymer aspects can be studied in detail. The study also shows that the introduction of specific groups at the tips of the backbone, or probably even more efficiently at the ends of short side chains, can lead to a surface functionality, such as strong specific adhesion, which could be of high practical relevance.

Acknowledgment. We are grateful to C. F. Abrams, M. Parrinello, A. Alavi, and R. O. Jones for many helpful comments and suggestions. The work was supported by the Bundesministerium für Bildung and Forschung (the German Federal Ministry of Education and Research), grant No.03 N 6015 on materials simulations.

Appendix: Details of the Ab Initio Study of Carbonic Acid and Propane on Ni(111)

We use the code FEMD of Alavi et al.[37,38] implemented in the CPMD code.[36] In this DFT-based finite-electronic temperature method, the electron density and the Hellmann−Feynman forces are computed using a subspace diagonalization of a high-temperature density matrix within a self-consistent procedure. The subspace is expanded in a plane-wave basis set, up to a cutoff of 60 Ry. A partial occupation of states at Fermi level can be handled, and *k*-point sampling of the electronic states in the Brillouin zone of the supercell is also implemented. The system consists of a carbonic acid molecule or a propane and a Ni(111) surface which is represented by four close-packed layers of Ni(111) (lattice parameter $a_0 = 3.543$ Å), with the top two layers (and the molecule) allowed to relax. We used a (2×2) lateral supercell in hexagonal symmetry of dimensions 5.01×5.01 Å^2, employing a $4 \times 4 \times 1$ *k*-point mesh, corresponding to 0.25 monolayer (ML) coverage. For the adsorption of propane, to estimate coverage-dependent effects, we performed additional calculations at a lower coverage of 0.11 ML, using a (3×3) lateral supercell; we found the same general adsorption behavior and a negligible difference in the adsorption energy ($E_{\mathrm{diff}} \approx 0.01-0.02$ eV) between the two coverages. The cell dimension in the *z*-direction was taken to be 20 Å, so that the amount of vacuum between the molecule and the bottom layer of the periodic image slab of Ni(111) was approximately 10 Å. A Troullier−Martins pseudopotential is used for oxygen and carbon,[39] a local pseudopotential is used for hydrogen,[40] and for nickel a soft kinetic-energy-filtered pseudopotential is used.[41] For each calculation, we used the PBE[42] generalized gradient approximation (GGA); in addition, for some calculations, we also used the Perdew−Becke[43] GGA. We compared the two functionals and noticed that results do change by a rather small amount in the adsorption energies (0.01 eV); the geometries do depend more sensitively on the functional. For propane, in the energetically most favorable geometry, a difference of ∼0.2 Å for the average equilibrium distance from the surface is found. Our general preference for the PBE functional stems from calculations of other relevant molecules on Ni(111) (benzene and phenol[35]), for which the PBE functional seems to give a more consistent picture. We tested our setting by performing test calculations for determining bulk and surface properties for nickel and by reproducing the geometry of the isolated molecule for carbonic acid and propane. Geometry optimizations of the molecules/surface system were performed using a quasi-Newton (BFGS) method. The starting orientations of the molecules were taken to be compatible with the geometric constraints imposed by a BPA-PC polymer chain. These orientations were taken as initial configurations for energy optimization. We checked that, after optimization, the final geometry of each molecule, as for the initial one, was compatible with the geometric constraints of the BPA-PC chain. The resulting adsorption energy characterizes the strength of the interaction of each submolecule with the surface.

A. Carbonic Acid. We selected molecular orientations with respect to the surface which are compatible with chain conformations at the surface. For each configuration, one should take into account four high-symmetry site locations above the surface and, possibly, different orientations of the molecule in the plane parallel to the surface. We found that, independent of the initial geometry, the molecule does not stick to the surface; that is, the molecule experiences the surface as a uniform repulsive wall. The most favorable configuration is the one where the molecule lies parallel to the surface at a distance of about 3.35 Å with a very small adsorption energy of about 0.01 eV which is negligible as compared to the inherent error of the GGA, and also smaller than the characteristic thermal energies in typical melt processing of polycarbonates that we intend to model (570 K, $k_{\mathrm{B}}T \approx 0.05$ eV). We carried out a detailed study of the dependence of the adsorption energy as a function of the distance from the surface; results are illustrated in Figure 4a. We build the energy curve by adiabatically moving the molecule from the optimal distance of 3.35 Å toward the surface and in the opposite direction along the *z*-axis. Starting from the optimal configuration, we shift the molecule along the *z*-axis (perpendicular to the surface) a small amount (about 0.2 Å), fix the *z*-coordinate of the carbon, and allow the molecule and the two top layers of Ni to relax. Once the forces have reached an average value which is below 1.0×10^{-3} au, we take this last optimized configuration and repeat the procedure again; each optimized geometry corresponding to a fixed carbon−surface distance represents a point in Figure 4a. To check the validity of the information given by Figure 4a, we repeated the process in a sort of inverse order; that is, we started, for different molecular orientations and at different relevant sites of the surface, with an initial molecule−surface distance of about 2.1 Å and did not fix the carbon, thus allowing the molecule to freely move in any direction. Results show that, independent of the initial geometry and surface site, the molecule experiences strong repulsion and finally ends up at distances which are very close to the optimal distance of about 3.35 Å, with adsorption energies of the order of 0.01 eV. These results, taking into account the energy scale involved in the polymer−surface problem, allow us to model the surface for the carbonate bead of the polymer as a uniform hard wall with a minimum bead−surface distance of about 3.2 Å.

B. Propane. We repeated for propane the same procedure adopted in the preceding case regarding carbonic acid. As for carbonic acid, we found that the molecule does not stick to the

(39) Troullier, N.; Martins, J. L. *Phys. Rev. B* **1991**, *43*, 1993.
(40) Gygi, F. *Phys. Rev. B* **1993**, *48*, 11692.
(41) Lee, M. H. Ph.D. Thesis, Cambridge University, 1995.
(42) Perdew, J. P.; Burke, K.; Ernzerhof, M. *Phys. Rev. Lett.* **1996**, *77*, 3865.
(43) Becke, A. D. *Phys. Rev. A* **1988**, *38*, 3098. Perdew, J. P. *Phys. Rev. B* **1986**, *33*, 8822.

surface and the optimal configuration is found to be one of the first kind with the center-of-mass−surface distance of about 3.9 Å corresponding to an energy of 0.03 eV for the lower coverage and 0.01 eV for the higher coverage. At about 3.2 Å, the repulsion starts to be significant with respect to the thermal energy of the polymer melt, see Figure 4b. To build the energy curve of Figure 4b and check its validity, we repeated the procedure adopted for carbonic acid; in this case, to allow the center of mass to have only small oscillations in the *z*-direction around a given position, we fixed the *z*-coordinate of the C3 atom. As for carbonic acid, the results for propane allow us to model the interaction between surface isopropylidene groups of the polymer as a uniform hard wall with a minimum bead−surface distance of about 3.2 Å.

JA0387406